C. R. Chimie 5 (2002) 431–440

S1631074802014066/FLA

Synthesis and characterisation of bite angle-dependent (η^1-allyl)Rh and (η^3-allyl)Rh complexes bearing diphosphine ligands. Implications for nucleophilic substitution reactions

Richard J. van Haaren, Erik Zuidema, Jan Fraanje, Kees Goubitz, Paul C.J. Kamer, Piet W.N.M. van Leeuwen*, Gino P.F. van Strijdonck

Institute for Molecular Chemistry, University of Amsterdam, Nieuwe Achtergracht 166, 1018 WV Amsterdam, The Netherlands

Received 18 March 2002; accepted 23 July 2002

Abstract – Several novel rhodium allyl complexes have been prepared and their structures have been studied using NMR spectroscopy and X-ray crystallography. Depending on the bite angle of the ligand and the substitution pattern of the allyl group, two different coordination modes (η^1 and η^3) have been observed for the allyl moiety. The activities of these Rh allyl complexes in the allylic alkylation reaction have been tested. We have shown that both coordination modes give active complexes in this reaction, but that the regioselectivity is dependent on the coordination mode of the allyl group. ***To cite this article: R.J. van Haaren et al., C. R. Chimie 5 (2002) 431–440*** © 2002 Académie des sciences / Éditions scientifiques et médicales Elsevier SAS

rhodium / allylic alkylation / crystal structure / homogeneous catalysis / regioselectivity

Résumé – Plusieurs nouveaux complexes allyl–rhodium ont été préparés et leurs structures étudiées par spectroscopie RMN et cristallographie aux rayons X. Suivant l'angle de « morsure » du ligand et le schéma de substitution du groupe allyle, deux modes de coordination différents (η^1 et η^3) ont été observés pour l'entité allylique. Les activités de ces complexes allyl–rhodium dans la réaction d'alkylation allylique ont été testées. Nous avons montré que les deux modes de coordination donnent des complexes actifs dans cette réaction, mais que la régiosélectivité dépend du mode de coordination du groupe allylique. ***Pour citer cet article : R.J. van Haaren et al., C. R. Chimie 5 (2002) 431–440*** © 2002 Académie des sciences / Éditions scientifiques et médicales Elsevier SAS

rhodium / alkylation allylique / structure cristalline / catalyse homogène / régiosélectivité

1. Introduction

The allylic substitution reaction (Fig. 1) is one of the most intensively studied catalytic reactions. Since the early reports by Tsuji [1–3] and Trost [4–6], it has become a powerful and versatile tool in synthetic organic chemistry. The reaction is compatible with a wide variety of allylic substrates as well as nucleophiles.

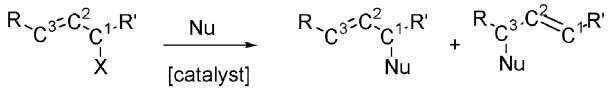

Fig. 1. The allylic substitution reaction.

Recent research mainly focuses on asymmetric reaction variants [7] using often cyclic or linear 1,3-disubstituted acetates. The use of small substituents on

* *Correspondence and reprints.*
E-mail address: pwnm@science.uva.nl (P.W.N.M. van Leeuwen).

the allyl moiety leads to less steric interaction between the ligand and the allyl group and consequently to a less efficient transfer of chiral information. Therefore, only ligands bearing the chiral centre in close proximity to the metal centre have been successful for such substrates [7, 8].

When mono-substituted allylic substrates such as cinnamyl (R=Ph, R'=H in Fig. 1) are used, regiocontrol is required prior to enantiocontrol. Palladium(bisphosphane) catalysts have been studied widely but show a preference for the formation of the linear product [9–11]. Using mixed donor atom bidentate ligands, the regioselectivity can be steered [12–15]. Recently it has been shown that catalysts based on metals such as tungsten [16], molybdenum [17], iridium [18–20] platinum [21, 22] and rhodium [23–25] show a preference for the chiral branched product, but the rate of the reaction is much lower than that observed for palladium.

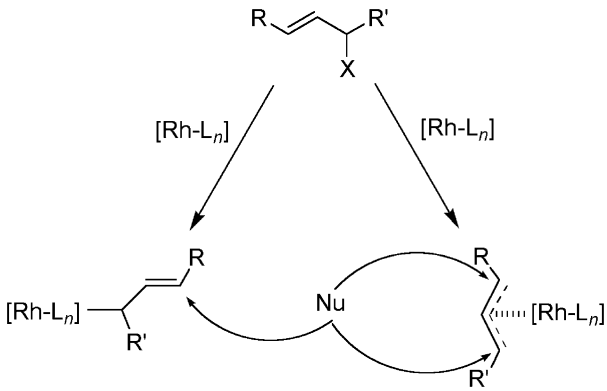

Fig. 2. The postulated S_N2' mechanism for the rhodium-catalysed allylic alkylation via a Rh(η^1-cinnamyl) species (left) and the alternative pathway via a Rh(η^3-cinnamyl) species (right).

Although the palladium-catalysed reaction is known to proceed via an η^3-allyl complex, for the rhodium system an η^1-allyl complex has been postulated as intermediate [23]. The alkylation on the η^1-allyl species will take place via an S_N2' attack of the nucleophile on the γ-carbon of the allyl moiety (Fig. 2). Alkylation of an allyl moiety with a substituent on the γ-carbon will yield the branched product.

The rhodium catalysts in the reported alkylation studies were prepared in situ using an excess of monodentate phosphine ligands. For these systems, η^1-allyl complexes have indeed been observed [26], but similar complexes bearing bidentate phosphine ligands have not been studied so far. In the late sixties, Vrieze [27] and the early eighties Fryzuk [28] have reported several studies concerning the synthesis and structure of allyl-rhodium complexes. Encouraged by their results we report here the synthesis and structure of novel (diphosphine)rhodium(allyl) complexes and evaluate their reactivity in the allylic alkylation reaction.

2. Results

2.1. Choice of ligands and allyl moieties

To study the effect of the bite angle of the ligand [29] on the geometry of (diphosphine)rhodium(allyl) complexes complex, four ligands having different preferred bite angles were used in this study (Fig. 3). Except for the ethanediyl bridged dppe (**2**), which enforces a relatively small bite angle and has a rather flexible backbone, the ligands are tri-aryl phosphines: *o*-dppb (**1**), which is a rigid ligand enforcing a small bite angle, DPEphos (**3**), which enforces an intermediate bite angle and has a flexible backbone and Xant-

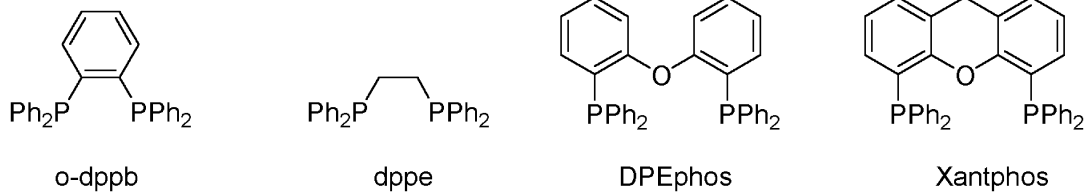

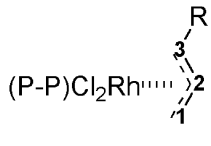

P-P	R=H	R=Ph
o-dppb	**1a**	**1b**
dppe	**2a**	**2b**
DPEphos	**3a**	**3b**
Xantphos	**4a**	**4b**

Fig. 3. Ligands and complexes used in this study.

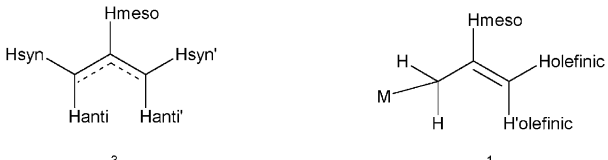

Fig. 4. Allyl coordination modes, η^3 (**a**) and η^1 (**b**).

phos (**4**), which enforces a large bite angle and has a more rigid backbone.

To study the effect of the substituent on the allyl moiety on the structure of the (diphosphine)rhodium(allyl) complexes, the small non-substituted C_3H_5 moiety (**a**) and the large phenyl substituted cinnamyl moiety (3-Ph–C_3H_4) (**b**) were used.

2.2. Synthesis

Starting from a Rh^I precursor, several routes were explored to synthesise (PP)Rh^{III}(allyl) complexes. The most convenient and versatile route proceeds via oxidative addition of the appropriate allyl chloride to (PP)Rh^I(COD)Cl, resulting in the dichloro complexes (PP)Rh^{III}(allyl)Cl_2. The oxidative addition reaction proceeds smoothly for all complexes. Only for the DPEphos complex **3a**, a small amount (< 5%) of an unidentified side product was formed that could not be removed.

2.3. Characterisation

An important issue in the characterisation of the newly synthesized Rh(allyl) complexes is the coordination mode (η^1- or η^3) of the allyl moiety. For palladium allyl complexes, the two coordination modes of the allyl moiety can be distinguished by several differences in the ^{1}H-NMR spectra. For Pd(η^3-allyl) complexes, the five hydrogens (Fig. 4) on the allyl moiety are non-equivalent in non-symmetrical complexes, whereas in symmetrical complexes {H_{anti} and $H_{anti'}$} and {H_{syn} and $H_{syn'}$} are equivalent.

The anti hydrogens are closer to palladium and show a signal at lower ppm-value than the syn-hydrogens. In general, the signal for H_{anti} is typically found between 2 and 3.5 ppm, whereas the signal for H_{syn} is mostly observed between 2.5 and 3.9 ppm. The signal of H_{meso} almost always appears above 5 ppm, but below 6.5 ppm. In some cases, the η^3-allyl moiety shows fluxional behaviour and H_{anti} and H_{syn} become equivalent via a η^3–η^1–η^3 rearrangement, which results in only one signal for the anti- and syn-hydrogens appearing at the averaged chemical shift.

The presence of a phenyl substituent at the allyl moiety (cinnamyl) disrupts the symmetry of the allyl group and all four protons show different signals. The phenyl can be oriented anti or syn with respect to H_{meso}. The signals of H_{anti} and H_{syn}, as compared to the C_3H_5 moiety, are in general shifted to a slightly higher ppm value. The chemical shift of the signal of the anti hydrogen next to the phenyl is found at lower field, because of the partial double bond character of the C2–C3 bond. The doublet may be observed even at higher chemical shift (between 5.9 and 6.8 ppm) than the signal of H_{meso}, which is found between 5.8 and 6.6 ppm.

So far, only few (η^1-C_3H_5)Pd complexes have been reported. The ^{1}H-NMR spectrum resembles that of organic allyl compounds e.g. allyl chloride [30–32]. The aliphatic CH_2-unit appears as one signal; the olefinic signals are magnetically non-equivalent. The fine structure and the chemical shift of the signal of H_{meso} resemble those found for H_{meso} in η^3-allyl complexes. The main difference, therefore, between an η^3- and an η^1-allyl is found in the fine structure on the signal of the olefinic CH_2-unit. The signal consists of two double doublets around 5 ppm, whereas this is not observed for the η^3-allyl complex.

The situation is slightly more complicated for cinnamyl complexes. In (triphos)Pd(η^1-cinnamyl)Cl the cinnamyl is bonded to the metal via the CH_2 unit, with a trans configuration of the allylic C=C bond. ((Triphos)Pd(η^1-cinnamyl)Cl: ^{1}H-NMR: δ = 2.3–2.6 (2 multiplets, 4H, backbone), 2.7 (m, 2H, Pd–CH_2), 3.0–3.3 (m(ddd), 4H, backbone), 5.1 (dd, J_1 = 15.3 Hz, J_2 = 5.6. Hz, 1H, =CH–Ph), 5.8 (dt, J_1(d) = 15.0 Hz, J_2(t) = 6.3 Hz, 1H, Pd–CH_2–CH= CH–Ph), 7.0–7.8 (m, 30 H, aromatic H); ^{31}P-NMR: δ = 47 (d, J = 48 Hz, 2P, –PPh_2), 99 (J = 48 Hz, 1P, PPh_2–P(Ph)–PPh_2); this palladium complex and other Pd(η^1-cinnamyl) complexes are not reactive in the stoichiometric and the catalytic allylic alkylation; unpublished results). The ^{1}H-NMR spectrum of these complexes shows one signal for the CH_2 unit, a multiplet for H_{meso} and a doublet for $H_{olefinic}$ ($H_{olefinic}$ is bonded to the terminal carbon atom). Thus, the spectra of Pd(η^1-cinnamyl) compounds are expected to be quite similar to those of an η^3-cinnamyl group, in which H_{anti} and H_{syn} are equivalent or rapidly exchanging. Contrary to the η^3-cinnamyl group, the η^1-cinnamyl moiety does not show a phosphorus coupling on the olefinic hydrogen next to the phenyl group. Another tool to distinguish between the two coordination modes is the difference between the chemical shift of H_{meso} and $H_{olefinic}$. In the η^3-allyl complex, the chemical shift of $H_{olefinic}$ is higher than that of H_{meso}, whereas in the η^1-allyl complex the chemical shift of the meso proton is higher than the olefinic proton.

We have used the similarities in the NMR spectra of the rhodium allyl complexes to the palladium com-

Table 1. Assignment of allyl coordination mode in $(C_3H_5)Rh(PP)Cl_2$ complexes.

Compound	PP ligand	Hapticity	Resonances in ^{31}P-NMR	Remarks
1a	*o*-dppb	η^1	1	
2a	dppe	η^1	1	
3a	DPEphos	η^3	2	all hydrogens non-equivalent
4a	Xantphos	η^3	1	broad ^{31}P-NMR signal

plexes to assign the structure of the rhodium complexes (Tables 1 and 2). The interpretation of the ^{1}H-NMR spectrum of the *o*-dppb cinnamyl complex **1b** is hampered by the overlap of $H_{olefinic}$ and the aromatic hydrogens. Because of the similarities between the NMR spectra of **1b**, **1a** and **2b**, the signals have been assigned to an η^1-cinnamyl moiety. In addition, the Xantphos bearing complex, **4b**, binds the cinnamyl in an η^1-fashion. Both DPEphos modified complexes, **3a** and **3b**, have been identified as η^3-allylic complexes.

In most complexes, the two phosphorus atoms show only one signal in the ^{31}P-NMR spectra, which is indicative of a symmetric complex geometry. Rhodium(III) can adopt several geometries: octahedral, square pyramidal, and trigonal bipyramidal. Although the coordination mode of the allyl is clearly identified by ^{1}H-NMR, the geometry around the rhodium is not resolved. Since the chemical shift of ^{103}Rh is known to be dependent on the geometry around the metal centre, attempts were made to measure the ^{103}Rh-NMR signal. Unfortunately, the signals were too broad to be conclusive, even at low temperature.

After recrystallization of (Xantphos)Rh(Cl_2)(η^3-C_3H_5) **4a** from CH_2Cl_2/hexane, crystals were obtained that were suitable for X-ray crystallography (Fig. 5). The structure of **4a** is similar to the crystal structure of the analogous cationic (Xantphos)Pd(η^3-C_3H_5)OTf [33]. Geometrical data of both complexes are presented in Table 3.

The rhodium complex has an octahedral structure, with the two chloride ligands in the axial positions, the two phosphine atoms cis to one another and the allyl in the equatorial plane bonded in an η^3-fashion. In contrast to the palladium complex, the rhodium complex has no C_S symmetry, probably because of the non-symmetric π–π interactions between the phenyl rings of the ligand. Compared to the palladium complex, the metal to allyl distance is larger and the C–C bonds in the allyl moiety are longer. Although the longer C–C bonds may suggest less olefinic character of the allyl moiety, the C–C–C angle of the allyl is larger. In addition, the angle between the P–M–P plane and the allyl C–C–C plane is much smaller. The coordination mode of the allyl group may thus indicate a decreased bonding and an increased backbonding interaction compared to the palladium complex. The P–Rh–P bite angle is similar to the calculated natural bite angle and to the bite angle found in other rhodium complexes of Xantphos derivatives [29].

The perpendicular stacking of the phenyl rings may explain the low chemical shift in the ^{1}H-NMR spectrum (1.2 ppm) of one of the multiplet signals of the CH_3 groups of the ligand. A different orientation of

Table 2. Assignment of allyl coordination mode in (3-Ph-C_3H_4)Rh(PP)Cl_2

Compound	PP ligand	Hapticity	Resonances in ^{31}P-NMR	Remarks
1b	*o*-dppb	probably η^1	1	$H_{olefinic}$ under aromatic signals
2b	dppe	η^1	1	
3b	DPEphos	η^3	2	broad signals in ^{1}H-NMR
4b	Xantphos	η^1	1	

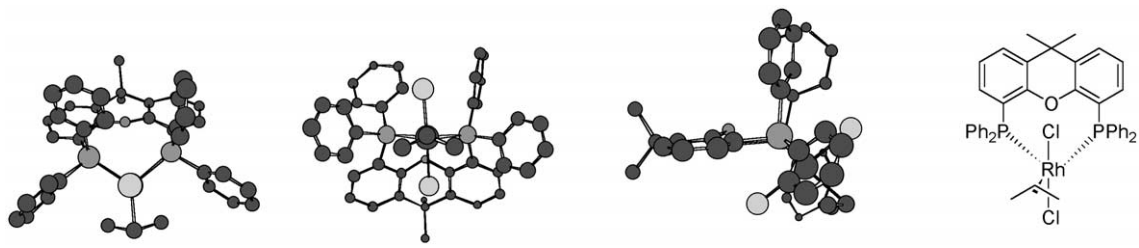

Fig. 5. Crystal structure of complex **4a** (three points of view and one schematic representation).

Table 3. Selected geometrical data of the crystal structures of (Xantphos)Rh(Cl_2)(η^3-C_3H_5) (**4a**, Fig. 5) and (Xantphos)Pd(C_3H_5)$^+$ OTf^- [33]. Distances in Å, angles in degrees (°). C1–C3 are the allylic carbon atoms, P1 is cis to C1, Cl1 is above in Fig. 4, Cl2 is below in Fig. 4.

	Rhodium	Palladium
d(M–C1)	2.232(11)	2.17(1)
d(M–C2)	2.186(14)	2.16(1)
d(M–C3)	2.241(11)	2.17(1)
d(C1–C2)	1.414(18)	1.34(2)
d(C2–C3)	1.442(18)	1.34(2)
∠(C1–C2–C3)	124.9(14)	120.4(15)
d(M–P1)	2.394(2)	2.372(2)
d(M–P2)	2.437(2)	2.372(2)
d(Rh–Cl1)	2.351(3)	
d(Rh–Cl2)	2.363(2)	
∠(P–M–P)	106.89(7)	108.11(7)
∠(Cl–Rh–Cl)	177.44(10)	
angle between xanthene planes	16.6571	27.352
d(M–O)	3.320(6)	3.445(7)
∠((P–M–P)–(C1–C2–C3))	58.9154	99.368
d(C1–(P–M–P))	–0.2723 (below)	+0.349
d(C2–(P–M–P))	+0.3136	+1.008
d(C3–(P–M–P))	–0.2195	+0.349

the phenyl rings causes a different folding of the Xanthene backbone and also a different ring current experienced by the methyl groups. Because of the large folding of the Xanthene backbone in the rhodium complex **4a**, the difference between the endo and exo methyl group is smaller than in the analogous palladium complex.

2.4. Allylic alkylation

The rhodium allyl complexes **1b**, **4a**, **4b** and the palladium analogue of **4b,** (Xantphos)Pd(C_3H_5)$^+$ have been used in the stoichiometric and catalytic alkylation using sodium diethyl 2-methylmalonate as the nucleophile. The results concerning the regioselectivity are shown in Tables 4 and 5. Since the rhodium-catalysed reactions proceed more slowly than the palladium-catalysed reactions, the former reactions are conducted using more concentrated reaction mixtures.

The stoichiometric and the catalytic reactions show that probably both η^3- and η^1-allyl complexes are alkylated. In the stoichiometric alkylation, the regioselectivity for the formation of the branched product (nucleophilic attack at the substituted C^3, see Fig. 1) is high for the *o*-dppb complex **1b** (88%), whereas the Xantphos complex **4b** shows a preference for the linear product and only 23% of the branched product is observed. Nevertheless, the selectivity to the branched product found using **4b** is significantly higher than that found using its palladium analogue (Xantphos)(cinnamyl)OTf (8%). In the *catalytic* reaction of complex **4b**, the same regioselectivity is found as in the stoichiometric reaction, suggesting that the reaction proceeds via the same pathway. Using the Xantphos rhodium complex, the reaction proceeds faster for allyl chloride than for cinnamyl chloride and at a rate similar to that of the palladium complex.

Table 4. Stoichiometric alkylation of allyl complexes using sodium diethyl 2-methylmalonate as the nucleophile (100% yield, for reaction conditions: see experimental section).

Complex	Branched (%)*	Linear (%)*
1b (*o*-dppb) (cinnamyl)	88	12
4b (Xantphos) (cinnamyl)	23	77
4a (Xantphos) (allyl)		100
Pd(Xantphos)(cinnamyl)OTf	8	92

* The branched product is formed from attack at the substituted C^3 atom and the linear product is obtained from attack at the non-substituted C^1 atom (see Fig. 1, R = phenyl, R' = H).

3. Discussion

3.1. Structures

For the rhodium allyl complexes with the smaller bite angle ligands (*o*-dppb and dppe), we obtained complexes in which the allyl moiety is coordinated in a η^1-fashion. Although it can be expected that an octahedral structure is favoured for complexes having small bite angle ligands, such a coordination may put too much strain on the backbone of the ligand or may cause too much steric hindrance for the substituents on the phosphorus atom. Therefore, the geometry around the rhodium(*o*-dppb) and rhodium(dppe) are distorted. This distortion could explain the formation of η^1-complexes for these ligands.

NMR spectroscopy shows that for DPEphos, both rhodium allyl complexes **3a** and **3b** are η^3-allyl structures with most likely an octahedral geometry. The NMR studies show, that in contrast to the other ligands, the two phosphorus atoms of the C_3H_5 complex **3a** are not equivalent, which indicates that the Rh-allyl bond is not symmetric. This has been observed before in crystal structures of cationic (DPEphos)Pd(allyl) complexes [33]. It appeared that the backbone of the DPEphos ligand is folded, such that one of the aromatic rings of the backbone has a π–π interaction with one of the phenyl rings of the phosphorus atom that is bonded to the other backbone ring.

According to NMR spectroscopy, the Xantphos complexes **4a** and **4b** differ in structure and presumably also in the geometry around the rhodium. The crystal structure clearly shows an octahedral geometry

Table 5. Catalytic allylic alkylation using sodium diethyl 2-methylmalonate as the nucleophile (for reaction conditions: see experimental section).

Complex	TOF_{ini}*	% Conversion**	Branched (%)**	Linear (%)**
4a (allyl)	107	44	100	
4b (cinnamyl)	15	13	21	79

* Determined after 45 min. ** Determined after 4 h; the branched product is formed from attack at the substituted C^3 atom and the linear product is obtained from attack at the non-substituted C^1 atom (see Fig. 1, R = phenyl, R' = H).

for **4a**, but for the η^1-complex **4b** calculations predict a square pyramidal complex [34]. It is not clear whether the two phosphorus atoms are cis or trans to one another. A trans coordination of Xantphos, with a coordinated oxygen, has been observed in *cationic* palladium complexes [35] but seems less likely in a *neutral* rhodium complex. We therefore propose a cis coordination of the Xantphos ligand in complex **4b**. The different coordination behaviour of C_3H_5 and cinnamyl to the rhodium is presumably caused by steric hindrance. In our previous work, it was described that a large cone angle of the ligand influences the coordination of the allyl group [33]. A strong steric interaction between Xantphos and the cinnamyl moiety may therefore cause the different coordination behaviour observed in compounds **4a** and **4b**.

3.2. Allylic alkylation

It has been suggested that, in contrast to palladium, rhodium allyl complexes react via an S_N2' attack on the γ carbon of the η^1-allyl moiety. We found that both η^1- and η^3-complexes react with sodium diethyl 2-methylmalonate to form the corresponding alkylated products indicating that both mechanisms are feasible for rhodium allyl complexes. Attack on the substituted γ-carbon of the η^1-cinnamyl of *o*-dppb complex **1b** results in a high regioselectivity for the branched product (88%). Remarkably, the alkylation of the analogous Xantphos η^1-complex **4b** results in the formation of only 23% of the branched product. This relatively low regioselectivity could be explained by a nucleophilic attack on an η^3-allyl moiety (S_N2) rather than substitution via an S_N2' mechanism. Possibly, complex **4b** undergoes a rearrangement from η^1 to η^3 in the reaction mixture. The increased polarity of the solution and an interaction between the sodium of the nucleophile and a chloride of **4b** may cause the formation of an intermediate rhodium complex with an enlarged Rh–Cl distance, which would enhance the possibility of η^3-coordination of the cinnamyl group. The possibility of nucleophilic attack on a rhodium allyl complex is evidenced by the successful reaction between the η^3-allyl complex **4a** and malonate. If **4b** reacts via the η^3-structure, the higher selectivity for the branched product (23%) relative to the palladium analogue Pd(Xantphos)(cinnamyl)OTf (8%) can be explained by the large distortion of the Rh–cinnamyl bond (see above).

The catalytic alkylation of cinnamyl chloride using complex **4b** shows the same regioselectivity as in the stoichiometric reaction, which indicates that the reactions proceed via the same intermediate. The alkylation of cinnamyl chloride using **4b** proceeds relatively fast, even compared to palladium-catalysed allylic alkylation. The high reaction rate observed for complex could be explained by instability of an intermediate η^3-cinnamyl complex and the large distortion of the Rh-cinnamyl bond. Furthermore, modelling studies [34] showed that for the η^3-allyl complex, the backbonding interaction might be relatively small compared to the analogous palladium complex. We have shown that a smaller backbonding interaction enhances the reactivity towards nucleophilic attack [34, 36]. The overall regioselectivity may therefore be a result of a competition between the S_N2' mechanism and the η^3-mechanism. For η^3-complexes, a larger bite angle of the ligand will result in an increase of the reactivity and the η^3-mechanism may be favoured over the S_N2' mechanism.

4. Conclusion

We have synthesised and isolated a series of novel Cl_2Rh^{III}(diphosphine)allyl complexes. The coordination mode of the allyl moiety (η^1 or η^3) is highly dependent on the ligand and the substituents on the allyl moiety. The Rh(allyl) complexes react with malonate to form the alkylated product. The nature of the rhodium-allyl bond influences the mechanism of this reaction. In the allylic alkylation, an η^1-complex reacts via the S_N2' mechanism whereas an η^3-complex reacts via nucleophilic attack on the η^3-allyl moiety. For palladium complexes, the η^3-allyl square planar cationic geometry is favoured, whereas the crystal structure of **4a** shows that neutral penta-coordinated complexes are formed for rhodium. The possibility for rhodium to adopt different geometries facilitates the formation of η^1-allyl complexes. For palladium, η^1-allyl complexes can only be formed when using tridentate ligands and coordinating counterions, and these η^1-allyl species have shown to be non-reactive towards nucleophiles. In contrast, η^1- and η^3-allyl

rhodium complexes described in this chapter react readily to form the alkylation product with a moderately high regioselectivity for the chiral, branched product.

5. Experimental section

5.1. General remarks

All reactions were performed in an atmosphere of argon unless stated otherwise. Dichloromethane was distilled under nitrogen atmosphere from P_2O_5; pentane, hexane, and toluene were distilled from sodium, THF, and diethyl ether from sodium/benzophenone. Bis-1,2-(diphenlylphoshino)-ethane and bis-1,2-(diphenylphoshino)-benzene were purchased from Aldrich and used as received. Xantphos and DPEphos were prepared according to a literature procedure [37]. Allylchloride and cinnamylchloride were obtained from ACROS and used as received. $[Rh(COD)Cl]_2$ was synthesised according to a literature procedure [38].

The stoichiometric alkylation reactions were performed by adding an excess of sodium diethyl 2-methylmalonate (0.1 ml of a 0.5 M solution in THF) to a solution of 10 mg of the Rh-complex in 1 ml of THF. Reaction was instantaneous and after one minute, the mixture was worked up with water, filtered over silica, and analysed by GC.

The catalytic reactions were performed in THF (10 ml), using 0.5 mol% of catalyst (0.0050 mmol), 1.0 mmol of 3-Me-but-2-enyl acetate and 2.0 mmol of sodium diethyl 2-methylmalonate. The reaction was monitored by taking samples from the reaction mixture, which after quenching with wet ether, were analysed by GC using decane as the internal standard.

^{1}H-, ^{31}P{^{1}H}- and ^{13}C–NMR spectra were recorded at 300, 121 and 75 MHz respectively on a Varian FT NMR spectrometer. Variable temperature NMR experiments were performed on a Brucker DRX-300 FT NMR spectrometer equipped with a variable temperature unit. Chemical shifts are reported in δ units (ppm) and referenced to the residual deuterated solvent signal for ^{1}H- and ^{13}C–NMR spectroscopy, external H_3PO_4 (δ = 0 ppm) for ^{31}P{^{1}H}-NMR spectroscopy. The numbering scheme for the allyl moiety is shown in Fig. 4.

5.2. Rh(DPPE)(COD)Cl

16.1 mg of $[Rh(COD)Cl]_2$ (0.06 mmol) was dissolved in 5 ml of THF. To this solution, 26.5 mg of DPPE (0.06 mmol, 97%) was added while stirring. The solution was stirred for 30 min. The solvent was removed in vacuo and the solid was washed twice using 10 ml of pentane.

^{1}H-NMR (CD_3CN): δ = 8.0–7.0 (20H, m, aromatic protons DPPE), 4.1 (4H, bs, olefinic protons COD), 3.5 (2H, m, backbone protons DPPE), 2.3 (4H, bs, aliphatic protons COD), 2.1 (2H, m, backbone protons DPPE), 1.7 (4H, bs, aliphatic protons COD).

^{31}P{^{1}H}-NMR (CD_3CN): δ = 63 (d, J(Rh,P) = 133 Hz).

5.3. Rh(Xanthphos)(COD)Cl

25 mg of $[Rh(COD)Cl]_2$ (0.05 mmol) was suspended in 5 ml of dry ether. To this suspension 58 mg of Xantphos was added as a finely ground solid. After addition, the solution was stirred for 30 min at room temperature, during which an orange solid precipitated. The orange solid was washed twice using 20 ml of ether. The product was dried under vacuum.

^{1}H-NMR (toluene-D_8): δ = 8.0–7.0 (26H, m, aromatic protons Xantphos), 4.5 (4H, bs, olefinic protons COD), 1.9 (4H, bs, aliphatic protons COD), 1.6 (6H, bs, methyl-protons Xantphos), 1.3 (4H, bs, aliphatic protons COD).

^{31}P{^{1}H}-NMR (toluene-D_8): δ = 7.6 (d, ^1J(Rh,P) = 91 Hz).

5.4. Rh(C_3H_5)(*o*-DPPB)Cl_2 1a

50 mg of $[Rh(COD)Cl]_2$ (0.10 mmol) were suspended in 5 ml of toluene. To this suspension, 90.1 mg of *o*-di(diphenylphoshino)-benzene (0.20 mmol) in 15 ml of toluene was added dropwise.

After addition, the solution was stirred for 1 h, during which the product precipitated as an orange solid. 0.05 ml of allylchloride (0.65 mmol) was added. The mixture was stirred for another hour at room temperature, during which the colour of the suspension changed from orange to yellow. 15 ml of pentane were added to facilitate precipitation. The liquids were removed and the solid was washed twice using 20 ml of pentane. The solid was dried under vacuum.

^{1}H-NMR ($CDCl_3$): δ = 8.0–6.2 (24H, m, aromatic protons *o*-DPPB), 5.1 (1H, m, H_{meso}), 5.0 (1H, dt, J(H,2H) = 4 Hz; J(H,H) = 14 Hz; $H'_{olefinic}$), 4.9 (1H, dt, J(H,2H) = 3 Hz; J(H,H) = 6Hz, $H_{olefinic}$), 2.6 (2H, d, J(H,H) = 8 Hz, H).

^{31}P{^{1}H}-NMR ($CDCl_3$): δ = 62 (bd, J(Rh,P) = 124 Hz).

HR–MS (FAB): $C_{33}H_{29}Cl_2P_2Rh^+$ requires m/z = 660.0176, found: 625.0491 (loss of one Cl).

5.5. Rh(C_3H_5)(DPPE)Cl_2 2a

29 mg of Rh(DPPE)(COD)Cl (0.05 mmol) were dissolved in 5 ml of THF. To this suspension, 0.05 ml of allylchloride (0.65 mmol) was added dropwise. The mixture was stirred for 30 min at room temperature.

The solvent was removed in vacuo and the product was washed twice using 10 ml of pentane. The yellow product was dried in vacuo.

^{1}H-NMR ($CDCl_3$): δ = 8.0–7.0 (20H, m, aromatic protons DPPE), 5.0 (1H, m, H_{meso}), 4.8 (2H, m, $H_{olefinic}$), 3.1 (2H, m, backbone protons DPPE), 2.9 (2H, bs, H), 2.5 ppm (2H, m, Backbone protons DPPE).

^{31}P{^{1}H}-NMR ($CDCl_3$): δ = 66 (bd, J(Rh,P) = 105 Hz).

5.6. Rh(DPEphos)(C_3H_5)Cl_2 3a

25 mg of $[Rh(COD)Cl]_2$ (0.05 mmol) were suspended in 5 ml of dry ether. 55 mg of DPEphos (0.10 mmol) was added as a finely ground solid to this suspension. After addition, the solution was stirred for 30 min at room temperature, during which a red solid precipitated. The solid was washed twice using 20 ml of ether. This solid was then suspended in 3 ml of THF. To this suspension, 0.05 ml of allylchloride (0.65 mmol, a large excess) was added dropwise. The mixture was stirred for 2 h, during which the colour of the solution changed from red to yellow and finally a yellow solid precipitated. The liquid was removed and the solid was washed twice using 20 ml of pentane. The solid was dried under vacuum.

^{1}H-NMR ($CDCl_3$): δ = 8.5–6.0 (aromatic protons DPEphos), 5.3 (1H, m, H_{meso}), 4.5 (1H, dd, J(H,H) = 13 Hz, J(H,H) = 10 Hz, H_{syn}), 4.2 (1H, dd, J(H,H) = 7 Hz, J(H,H) = 7 Hz, $H_{anti'}$), 3.1 (1H, d, J(H,H) = 7 Hz, $H_{syn'}$), 3.0 (1H, d, J(H,H) = 12 Hz, H_{anti}).

^{31}P{^{1}H}-NMR ($CDCl_3$): δ = 30 (1P, dd, J(Rh,P) = 115 Hz, J(P,P) = 9 Hz), 12 (1P, dd, J(Rh,P) = 144 Hz, J(P,P) = 9 Hz).

HR–MS (FAB): $C_{39}H_{33}Cl_2OP_2Rh^+$ requires m/z = 752.0439, found: 717.0755 (loss of one Cl).

5.7. Rh(Xanthphos)(C_3H_5)Cl_2 4a

42 mg of Rh(Xantphos)(COD)Cl (0.05 mmol) was suspended in 5 ml of toluene. 0.1 ml of allylchloride (1.3 mmol, a large excess) was added to this suspension. The reaction mixture was stirred for 2 h at room temperature. The solvent was removed in vacuo, and the product was dried under high vacuum (5×10^{-5} mbar).

^{1}H-NMR ($CDCl_3$): δ = 8.0–7.0 (26H, m, aromatic H's Xantphos), 5.5 (1H, p, J(H,4H) = 11 Hz, H_{meso}), 3.6 (4H, bs, $H_{anti} + H_{syn} + H_{syn'} + H_{anti'}$), 1.5 (6H, bs, CH_3's Xantphos).

^{31}P{^{1}H}-NMR ($CDCl_3$) : δ = 5 (bs).

HR–MS (FAB): $C_{42}H_{37}Cl_2OP_2Rh^+$ requires m/z = 792.0752, found: 757.1068 (loss of one Cl).

5.8. Rh(C_3H_4Ph)(*o*-DPPB)Cl_2 1b

49.2 mg of $[Rh(COD)Cl]_2$ (0.10 mmol) was suspended in 5 ml of toluene. To this solution, 90.1 mg of *o*-di(diphenylphoshino)-benzene (0.20 mmol) in 15 ml of toluene was added dropwise. After addition, the solution was stirred for 1 h, during which the product precipitated as an orange solid. 0.10 ml of cinnamylchloride (1.3 mmol, a large excess) was added. The mixture was stirred for 2 h at room temperature. 15 ml of pentane were added to facilitate precipitation. The liquids were removed and the solid was washed twice using 20 ml of pentane. The solid was dried under vacuum.

^{1}H-NMR ($CDCl_3$): δ = 8.0–7.0 (30H, m, aromatic protons *o*-DPPB and phenyl cinnamyl-group), 5.6 (1H, dt, J(H,H) = 8 Hz, J(H,2H) = 11 Hz, H_{meso}), 2.3 (2H, d, J(H,H) = 11 Hz, H).

^{31}P{^{1}H}-NMR ($CDCl_3$): δ = 64 (d, J(Rh,P) = 164 Hz).

5.9. Rh(DPPE)(C_3H_4Ph)Cl_2 2b

28 mg of Rh(DPPE)(CO)Cl (0.05 mmol) was dissolved in 5 ml of THF. To this solution, 0.05 ml of cinnamylchloride (0.65 mmol, a large excess) was added dropwise. The mixture was stirred for 30 min at room temperature. The solvent was removed in vacuo and the product was washed twice using 10 ml of pentane. The yellow product was dried in vacuo.

^{1}H-NMR ($CDCl_3$): δ = 8.0–7.0 (25H, m, aromatic protons DPPE and phenyl protons cinnamyl), 6.1 (1H, d, J(H,H = 25 Hz, $H'_{olefinic}$), 5.7 (1H, dt, J(H,H) = 25 Hz, J(H,2H) = 8 Hz, H_{meso}), 4.5 (2H, d, J(H,H) = 8 Hz, H), 3.3 (2H, m, backbone protons DPPE), 2.3 (2H, m, backbone protons DPPE).

^{31}P{^{1}H}-NMR ($CDCl_3$): δ = 69 (d, J(Rh,P) = 145 Hz).

5.10. Rh(DPEphos)(C_3H_4Ph)Cl_2 3b

25 mg of $[Rh(COD)Cl]_2$ (0.05 mmol) were suspended in 5 ml of dry ether. To this suspension, 55 mg of DPEphos (0.10 mmol) were added as a finely ground solid. After addition, the solution was stirred for 30 min at room temperature, during which a red solid precipitated. The solid was washed twice using 20 ml of ether. This solid was then suspended in 3 ml of toluene. To this suspension, 0.1 ml of cinnamylchloride (0.66 mmol, a large excess) was added. The solution was stirred at room temperature for 2 h. The product was precipitated using 20 ml of pentane. The liquids were removed, and the solid was washed twice, using 20 ml of pentane. The product was dried in vacuo.

^{1}H-NMR ($CDCl_3$): δ = 8.0–7.0 (33H, m, aromatic H's Xantphos and phenyl cinnamyl-group), 6.1 (1H,

bs, H_{syn}), 5.8 (1H, m, H_{meso}), 3.7 (1H, bs, $H_{syn'}$), 3.4 (1H, bs, $H_{anti'}$).

$^{31}P\{^{1}H\}$-NMR ($CDCl_3$): δ = 44 (1P, dd, J(Rh,P) = 180 Hz, J(P,P) = 15 Hz), 32 (1P, dd, J(Rh,P) = 134 Hz, J(P,P) = 15 Hz), 11 (0.1P, d, J(Rh,P) = 121 Hz, minor product).

5.11. Rh(Xantphos)(C_3H_4Ph)Cl_2 4b

40 mg of Rh(Xantphos)(COD)Cl (0.05 mmol) were suspended in 5 ml of toluene. To this suspension, 0.1 ml of cinnamylchloride (0.66 mmol, a large excess) was added. The reaction mixture was stirred for 2 h at room temperature. The solvent was removed in vacuo, and the yellow solid was washed twice using 10 ml of pentane. The product was dried under high vacuum (5×10^{-5} mbar).

^{1}H-NMR ($CDCl_3$): δ = 8.0–7.0 (31H, m, aromatic H's Xantphos and phenyl cinnamyl-group), 6.7 (1H, d, J(H,H) = 16 Hz, $H_{olefinic}$), 6.6 (1H, m, H_{meso}), 4.4 (2H, bs, H), 1.7 (6H, s, methyl-protons Xantphos).

$^{31}P\{^{1}H\}$-NMR ($CDCl_3$): δ = 16 (bd, J(Rh,P) = 117 Hz).

HR–MS (FAB): $C_{48}H_{41}{}^{35}Cl_2OP_2Rh^+$ requires m/z = 868.1065, found: 833.1384 (loss of one Cl).

5.12. Crystal structure determination of 4a

$C_{42}H_{37}Cl_2OP_2Rh$, M_w = 793.5, monoclinic, $P2_1/c$, a = 16.516(3) Å, b = 13.218(2) Å, c = 16.908(2) Å, β = 101.15(1)°, V = 3621.5(10) Å^3, Z = 4, Dx = 1.46 g cm^{-3}, λ(Cu Kα) = 1.5418Å, μ(Cu Kα) = 62.56 cm^{-1}, F(000) = 1624, room temperature, final R = 0.074 for 5558 reflections.

A crystal with dimensions $0.15 \times 0.20 \times 0.45$ mm approximately was used for data collection on an Enraf-Nonius CAD-4 diffractometer with graphite-monochromated Cu Kα radiation and ω–2θ scan. A total of 7453 unique reflections was measured within the range $-20 \le h \le 20$, $0 \le k \le 16$, $-21 \le l \le 0$. Of these, 5558 were above the significance level of 4 $\sigma(F_{obs})$ and were treated as observed. The range of (sin θ)/λ was 0.031–0.627Å ($2.7 \le \theta \le 75.3°$). Two reference reflections ([2 1 $\bar{4}$], [$\bar{2}$ 1 $\bar{1}$]) were measured hourly and showed no decrease during the 132-h collecting duration. Unit-cell parameters were refined by a least squares fitting procedure using 23 reflections with $39.91 \le \theta \le 41.00$. Corrections for Lorentz and polarisation effects were applied. Absorption correction was performed with the program PLATON [39], following the method of North et al. [40], using Ψ-scans of five reflections, with coefficients in the range 0.356–0.954. The structure was solved by the PATTY option of the DIRDIF99 program system [41]. The hydrogen atoms were calculated. Full-matrix least-squares refinement on F, anisotropic for the non-hydrogen atoms and isotropic for the hydrogen atoms keeping the latter fixed at their calculated positions with an atomic displacement parameter of U = 0.10 Å^2, converged to R = 0.074, R_w = 0.081, $(\Delta/\sigma)_{max}$ = 0.18, S = 1.07. A weighting scheme $w = [15 + 0.01 \times (\sigma(F_{obs}))^2 + 0.01/(\sigma(F_{obs}))]^{-1}$ was used. A final difference Fourier map revealed a residual electron density between –2.43 and 1.66 e Å^{-3} in the vicinity of the Rh. Scattering factors were taken from Cromer and Mann [42] and from the International Tables for X-ray Crystallography [43]. The anomalous scattering of Rh, P and Cl was taken into account [44]. All calculations were performed with XTAL3.7 [45].

References

[1] J. Tsuji, H. Takahashi, M. Morikawa, Tetrahedron Lett. (1965) 4387.

[2] J. Tsuji, Acc. Chem. Res. 2 (1969) 144.

[3] J. Tsuji, Tetrahedron 42 (1986) 4361.

[4] B.M. Trost, T.R. Verhoeven, J. Am. Chem. Soc. 98 (1976) 630.

[5] B.M. Trost, T.R. Verhoeven, J. Am. Chem. Soc 100 (1978) 3435.

[6] B.M. Trost, T.R. Verhoeven, in: G. Wilkinson, F.G.A. Stone, E.W. Abel (Eds.), Comprehensive Organometallic Chemistry, vol. 8, Pergamon, Oxford, 1982, pp. 799.

[7] B.M. Trost, D.L. Van Vranken, Chem. Rev. 96 (1996) 395.

[8] P. Dierkes, S. Ramdeehul, L. Barloy, A. De Cian, J. Fischer, P.C.J. Kamer, P.W.N.M. van Leeuwen, J.A. Osborn, Angew. Chem. Int. Ed. Engl. 37 (1998) 3116.

[9] M. Kranenburg, P.C.J. Kamer, P.W.N.M. van Leeuwen, Eur. J. Inorg. Chem. (1998) 25.

[10] J.D. Oslob, B. Åkermark, P. Helquist, P.O. Norrby, Organometallics 16 (1997) 3015.

[11] R. Kuwano, Y. Ito, J. Am. Chem. Soc. 121 (1999) 3236.

[12] R.J.H. van Haaren, H. Oevering, B.B. Coussens, G.P.F. van Strijdonck, J.N.H. Reek, P.C.J. Kamer, P.W.N.M. van Leeuwen, Eur. J. Inorg. Chem. (1999) 1237.

[13] R.J. van Haaren, C.J.M. Druijven, G.P.F. van Strijdonck, H. Oevering, J.N.H. Reek, P.C.J. Kamer, P.W.N.M. van Leeuwen, J. Chem. Soc. Dalton Trans. 10 (2000) 1549.

[14] R. Pretot, A. Pfaltz, Angew. Chem. Int. Ed. Engl. 37 (1998) 323.

[15] S. Vyskocil, M. Smrcina, V. Hanus, M. Polasek, P. Kocovsky, J. Org. Chem. 63 (1998) 7738.

[16] R. Pretot, G.C. Lloyd-Jones, A. Pfaltz, Pure Appl. Chem. 70 (1998) 1035.

[17] M.P.T. Sjogren, H. Frisell, B. Åkermark, O. Norrby P-, L. Eriksson, A. Vitagliano, Organometallics 16 (1997) 942.

[18] R. Takeuchi, M. Kashio, J. Am. Chem. Soc. 120 (1998) 8647.

[19] B. Bartels, G. Helmchen, Chem. Commun. (1999) 741.

[20] K. Fuji, N. Kinoshita, K. Tanaka, T. Kawabata, Chem. Commun. (1999) 2289.

[21] A.J. Blacker, M.L. Clark, M.S. Loft, J.M.J. Williams, Chem. Commun. (1999) 913.

[22] A.J. Blacker, M.L. Clark, M.S. Loft, M.F. Mahon, M.E. Humphries, J.M.J. Williams, Chem. Eur. J. 6 (2000) 353.

[23] P.A. Evans, J.D. Nelson, J. Am. Chem. Soc 12 (1998) 5581.

[24] P.A. Evans, J.E. Robinson, J. Am. Chem. Soc 123 (2001) 4609.

[25] P.A. Evans, L.J. Kennedy, J. Am. Chem. Soc.123 (2001) 1234.

[26] C.S. Chin, S.Y. Chin, C. Lee, J. Chem. Soc. Dalton Trans. (1992) 1323.

[27] H.C. Volger, K. Vrieze, J. Organomet. Chem. 9 (1967) 527.

[28] M.D. Fryzuk, Inorg. Chem 21 (1982) 2134.

[29] P.W.N.M. van Leeuwen, P.C.J. Kamer, J.N.H. Reek, P. Dierkes, Chem. Rev. 100 (2000) 2741.

[30] S. Ramdeehul, L. Barloy, J.A. Osborn, A. de Cian, J. Fischer, Organometallics 15 (1996) 5442.

[31] P.W. Blosser, M. Calligaris, D.G. Schimpff, A. Wojcicki, Inorg. Chem. Acta 320 (2001) 110.

[32] S. Ramdeehul, L. Barloy, J.A. Osborn, L. Carlotti, A. de Cian, J. Fischer, Eur. J. Inorg. Chem. (2000) 2523.

[33] R.J. van Haaren, K. Goubitz, J. Fraanje, G.P.F. van Strijdonck, H. Oevering, B. Coussens, J.N.H. Reek, P.C.J. Kamer, P.W.N.M. van Leeuwen, Inorg. Chem. 40 (2001) 3363.

[34] R.J.H. van Haaren, G.P.F. van Strijdonck, P.C.J. Kamer, P.W.N.M. van Leeuwen (manuscript in preparation).

[35] Y. Guari, G.P.F. van Strijdonck, P.C.J. Kamer, P.W.N.M. van Leeuwen, Chem. Eur. J. 7 (2001) 475.

[36] R.J. van Haaren, P.H. Keeven, L.A. van der Veen, K. Goubitz, G.P.F. van Strijdonck, H. Oevering, J.N.H. Reek, P.C.J. Kamer, P.W.N.M. van Leeuwen, Inorg. Chim. Acta 327 (2002) 108.

[37] M. Kranenburg, Y.E.M. van der Burgt, P.C.J. Kamer, P.W.N.M. van Leeuwen, Organometallics 14 (1995) 3081.

[38] G. Giordano, R.H. Crabtree, Inorg. Synth. 28 (1990) 84.

[39] A.L. Spek, Acta Crystallogr. Sect. A 46 (1990) 34.

[40] A.C.T. North, D.C. Phillips, F. Scott Mathews, Acta Crystallogr. Sect. A 26 (1968) 351.

[41] P.T Beurskens, G. Beurskens, R. Gelder de, S. Garcia-Granda, R.O. Gould, R. Israel, J.M.M. Smits, The DIRDIF-99 program system, Crystallography Laboratory, University of Nijmegen, The Netherlands, 1999.

[42] D.T. Cromer, J.B. Mann, Acta Crystallogr. Sect. A 24 (1968) 321.

[43] International Tables for X-ray Crystallography, Vol. IV, Kynoch Press Birmingham, 1974, p. 55.

[44] D.T. Cromer, D. Liberman, J. Chem. Phys. 53 (1970) 1891.

[45] S.R. Hall, D.J du Boulay, R. Olthof-Hazekamp (Eds.), XTAL3.7 System University of Western Australia, Lamb, Perth, 2000.